DOI: 10.13009/EUCASS2017-146

Liquid hydrogen low bond number reorientation: Experiment and numeric comparison

Philipp Behruzi
Airbus Safran Launchers
Airbus-Allee 1, D-28199 Bremen

Abstract

A reliable prediction of the physical phenomena of cryogenic propellants including phase change is of major interest to enable cost effective launcher developments. The availability of appropriate experimental microgravity data is crucial and for LH2 very hard to find. In the present paper experimental data obtained from drop tower tests using liquid hydrogen are being compared to numerical analyses. A quantitative comparison of the experiment is done. In conclusion it can be stated that the temperature evolution is qualitatively well captured. Further improvements are however necessary with respect to phase change and contact angle modelling.

1 Abbreviations

CFD	Computational Fluid Dynamics
LH2	Liquid hydrogen
PMD	Propellant Management Device
RCS	Reaction Control System
VoF	Volume of Fluid

2 Introduction

Considering future space missions, propellant management of cryogenic liquids in a microgravity environment is of strategic interest, e.g. for future space exploration including the anticipation of sending humans to Mars. Also present developments in Europe with respect to the Ariane 6 launcher require a thorough knowledge of the cryogenic liquid behaviour in space. Ballistic flight phases are part of the mission scenarios.

It is therefore one of the main points of interest to enable accurate predictions of boil-off rates throughout the mission. Propellant sloshing and liquid motions during the ballistic flight phases play a major role. Furthermore helium and vapour concentrations are of importance impacting the evaporation rate. The anticipation in becoming more profitable drives the need to develop analysis tools which are able to predict the phase change behaviour, especially the boil-off losses more accurately and reproducible in the future.

Cost effective developments of propellant tank concepts using cryogenic liquids will also desire as less functional development experiments as possible. This status, i.e. developing Propellant Management Devices (PMDs) by analysis-only, is today state-of-the-art for satellite tanks (see [1]). It is desirable to reach this status also for cryogenic liquids concerning boil-off and phase change. Analyses are generally done with Computational Fluid Dynamics (CFD) software tools.

Basis for evaluating and enhancing CFD tool capabilities are benchmark experiments. Microgravity experiments which consider cryogenic liquids are however expensive and therefore very sparse. Experiments were carried out mainly in drop towers or on sounding rockets (Maser 11 [2], Maser 12 [3], TEXUS 48 [4]). Maser 11 and 12 used HFE-7000 as test liquid representing phase change of cryogenic liquids. TEXUS 48 used LN2 as test liquid. In 2015 an additional experiment, named Cryofenix was launched using liquid hydrogen as liquid. No further information is however available.

DOI: 10.13009/EUCASS2017-146

Drop tower experiments are in comparison to sounding rockets much cheaper, however provide constraints with respect to the size of the experiment as well as concerning the duration of the drop. At ZARM, University of Bremen, the drop duration is about 4.7 seconds in comparison to roughly 6 minutes for TEXUS and MASER. Experiments may however be repeated allowing better parametric variations. Furthermore experiments may be tuned more accurately in drop tower tests also considering that the microgravity quality in the drop tower is excellent.

Drop tower experiments showing the reorientation of liquids in case of a step reduction from 1g to 0g were frequently done in the past, first with non-cryogenic liquids and then also with cryogenic liquids during the recent years. Kulev and Dreyer for example describe in [5] capillary driven surface oscillations of liquid argon at ambient pressure conditions. A partially filled circular cylinder was investigated considering non-isothermal boundary conditions. Oscillations were generated by the reorientation from a 1g surface condition to 0g during the drop of the capsule. This reorientation is the capillary dominated. The reorientation process is visualized in the following figure.

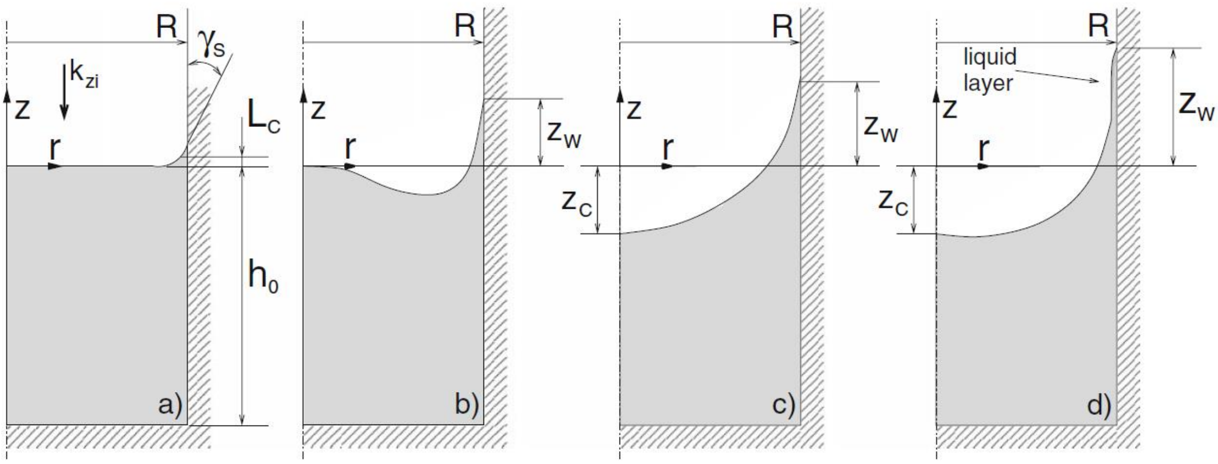

Figure 1: Reorientation process during step reduction in gravity from 1g to 0g: a) equilibrium condition in a 1g environment; b) - d) reorientation of the free surface in 0g (liquid phase in grey) [5]

The authors conclude that the reorientation process is strongly influenced by the temperature gradient in the wall which impacts the contact line behaviour preventing the formation of a liquid layer along the wall, depending on the temperature gradient.

Numerical analyses for the argon reorientation test were performed using the finite element solver NAVIER by the University of Erlangen [6]. The authors conclude in [7] that a qualitative agreement with the experimental results with liquid argon is given. A clear influence of the applied boundary condition on the interface reorientation is observed.

The reorientation in a spacecraft, e.g. after engine cut-off, may not be directly represented by this ideal configuration in the drop tower since the Bond number regimes may not be the same. The Bond number, representing the ratio of forces due to acceleration and the capillary forces, is expected to be much lower in the drop tower and thus much more capillary dominated then in the real flight configuration. Here RCS disturbances or residual tank motions including spin have to be considered. The motion in a flight tank is therefore generally much more complex. However concerning the validation of CFD tools the conditions in the drop tower are an optimum test condition allowing the detailed investigation of phase change phenomena.

In the present case the focus is therefore on drop tower experiments which involve cryogenic liquids using LH2. The experiments are detailed by Schmitt and Dreyer in [8] which will be recalled in the following chapter. The preceding chapter will then detail analyses which were carried out with our standard software FLOW-3D®. In this context it should be noted that most of the CFD analyses which were done were carried out with a rotational symmetric mesh, e.g. as discussed in [7]. However our goal is to consider numerical conditions which are as representative to our standard tank conditions as possible. In this context we did not consider rotational symmetric grids but a 3D mesh. Clearly this poses a strong constraint on the numerical analyses since the grid will be much coarser generally leading to higher inaccuracies.

DOI: 10.13009/EUCASS2017-146

3 Experiment conditions

Details concerning the benchmark experiment may be found in [8]. The present chapter summarizes the most important parameters and conditions which are needed to conduct a benchmark experiment. The geometry of the test dewar is depicted in the following figure.

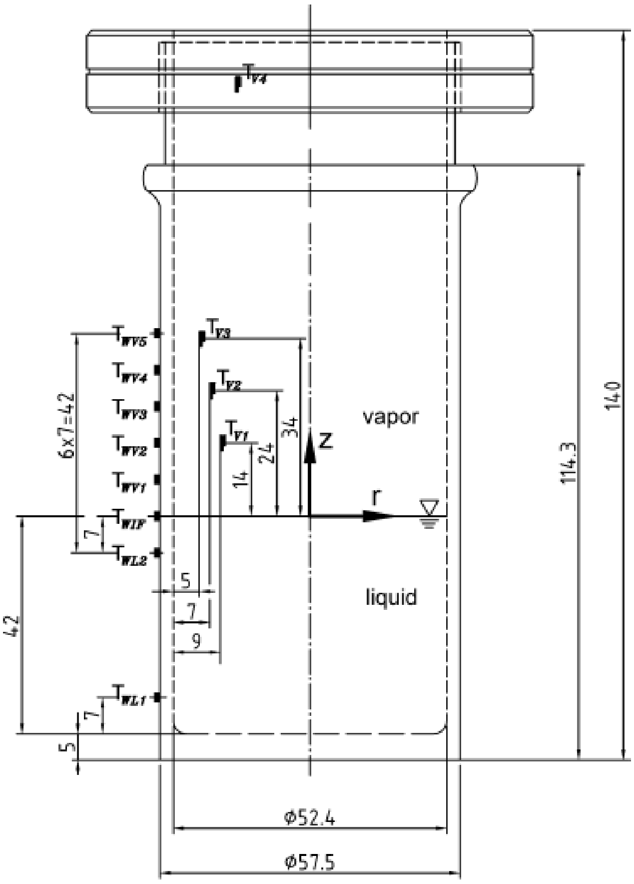

Figure 2: Geometrical conditions of the test dewar according to [8]

At t=0, before dropping the capsule and thus under 1g conditions, the free surface is located in the origin (z = 0mm) of the coordinate system filling the volume in negative z-direction. The dewar is made of borosilicate glass, embedded in a vacuum environment. Additional heat leaks into the dewar coming from outside are neglected. Properties of the dewar are listed in the following.

Table 1 Material properties of the borosilicate dewar. See also [9] for more information

Temperature (K)	Density (kg/m³)	Specific heat (J/(kg K))	Thermal conductivity (W/(m K))
20	2214	27.4	0.146
21	2214	30.6	0.15
22	2214	33.9	0.154
23	2214	37.3	0.158
24	2214	40.8	0.162
25	2214	44.3	0.167
26	2214	47.9	0.171

All other heat conducting elements were omitted in our simulation. For more information refer to [8]. Liquid properties of liquid Para hydrogen may be taken from the NIST database [10]. The liquid is initially at rest.

A number of temperature sensors are placed on the outside of the test dewar as well as inside the dewar in the gas phase.

DOI: 10.13009/EUCASS2017-146

- T_{WL1} & T_{WL2}: on the outside of the dewar at t=0 in the vicinity of the liquid phase
- T_{WIF}: on the outside of the dewar measuring at t=0 the liquid-gas interface temperature
- T_{WV1} - T_{WV5}: on the outside of the dewar at t=0 in the vicinity of the gas phase
- T_{V1} - T_{V4}: inside the dewar measuring at t=0 the gas temperature

Initial sensor temperatures considering two temperature profiles, cases 1 and 2, as well as the sensor positions are summarized in the following table.

Table 2 Temperature sensor locations, dedicated temperatures and ullage pressure conditions at t=0

	Sensor position		Case 1	Case 2
	z (mm)	r (mm)		
Ullage pressure p (Pa)			95005	72735
T_{WL1} (K)	-35	28.75	19.89	19.03
T_{WL2} (K)	-7	28.75	19.98	19.12
T_{WIF} (K)	0	28.75	20.06	19.20
T_{WV1} (K)	7	28.75	20.04	19.48
T_{WV2} (K)	14	28.75	20.03	19.85
T_{WV3} (K)	21	28.75	20.02	20.25
T_{WV4} (K)	28	28.75	20.13	20.76
T_{WV5} (K)	35	28.75	20.02	21.00
T_{V1} (K)	14	17.20	20.03	20.16
T_{V2} (K)	24	19.20	20.06	21.78
T_{V3} (K)	34	21.20	20.20	21.38
T_{V4} (K)	84	7.10	21.24	24.47

The absolute resolution of the sensors is ±0.25K. Furthermore it should be noted that the experiment data were corrected by about 0.3K taking into account that a laser which was switched on three to four times prior to the drop warmed up the temperature sensors. For more information refer to [8].

The dewar is connected via a piping to an external volume which is kept at ambient conditions, which however plays an essential role with respect to the pressure evolution during the drop test. The connected volumes are the following:
- Volume 1: 2.668 x 10^{-3} m³, homogeneous temperature at 300K
- Volume 2: 0.082 x 10^{-3} m³, expected to have a linear temperature gradient between 300K and the temperature of the test cell

The structures may be assumed adiabatic except the connections to the test cell.

4 Numerical setup and conditions

The two experiment cases 1 and 2 are the basis for the comparison with the numerical analysis. The following analyses were done:
1. Case 1: 1-fluid model isothermal. The experiment case 1 is considered to be in a saturated state. Thus, in order to compare the overall behaviour of the reorientation process, a standard 1-fluid model was chosen. The gas phase is neglected.
2. Case 1: 2-fluid model without consideration of phase change. Considering case 1 a 2-fluid model is used in comparison to the preceding 1-fluid model. Liquid as well as gas temperatures are taken into account.
3. Case 2: 2-fluid model without phase change but considering temperature changes. Phase change and temperature changes play a significant role for this test case. As a first step temperature changes only were taken into account neglecting phase change.
4. Case 2: 2-fluid model with phase change. In a following step also phase change physics was considered in the simulation.

The CFD software FLOW-3D® by Flow Science is used for the analyses. It is a standard software used to evaluate the propellant behaviour in spacecraft tanks using the Volume of Fluid (VoF) method. The mesh cells may then include fluid fractions of liquid, gas and solid. It is of interest to test this software with respect to the modelling of

DOI: 10.13009/EUCASS2017-146

cryogenic liquid behaviour including phase change. A 3D mesh was chosen in order to use similar models which would be also be applied for spacecraft tanks.

The computational domain is shown in Figure 3. A 90° wedge is calculated considering symmetry boundary conditions on the symmetry surfaces. The heat conduction in the borosilicate dewar is taken into account. Heat condition is set to zero for all other solid structures.

The minimum considered cell size is 0.5mm in the region of the dewar and 10cm maximum in the upper part of the computational domain (see figure below). For simplicity the computational domain was extended in vertical direction such that the considered volume of the gas phase is kept in accordance to the given values. A linear temperature rise was furthermore chosen, deviating from the proposed but not measured temperature profile. It is expected that temperature changes during the drop of about 4.7 seconds will not be impacted by temperature changes of the connected volumes.

2D view complete computational area	3D view of computational area before pre-run at 1g (t = 0s)	3D view of computational area after pre-run at 1g (t = 0.25s)

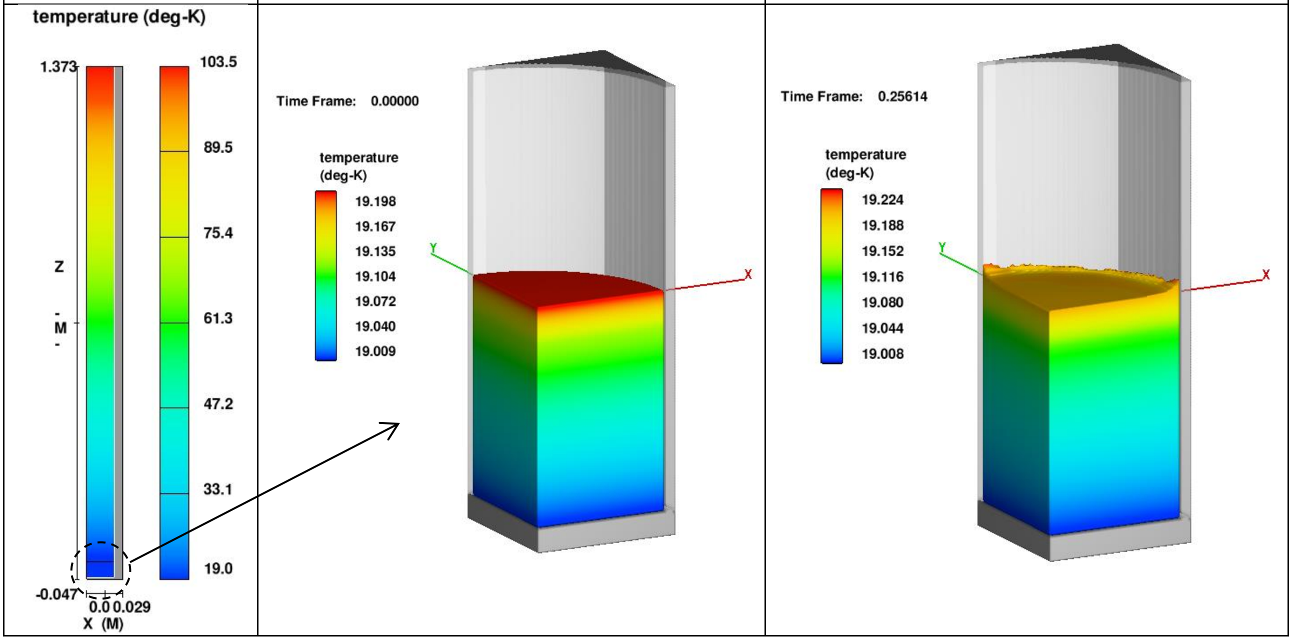

Figure 3: Initial condition of the temperature profile considering a 90° wedge of the dewar.

In the following a summary of the numerical settings are given for the 2-fluid model:

- Two fluids volume advection model with sharp interfaces
- 2nd order monotonicity preserving momentum advection
- Implicit GMRES pressure solver
- Two-fluid velocity slip model
- Two-fluid temperature slip model
- Two-fluid phase change model with accommodation coefficient α =0.001 for case 2. For comparison also α =0 was considered.
- No phase change for case 1; α =0
- 2nd order monotonicity preserving approximation to density transport equation
- Two-equation (k-e) turbulence model
- No slip model
- 0° contact angle
- Hertz-Knudsen phase change model for case 2 [11]
- 0g gravity conditions
- Rectangular mesh
- Temperatures sensors are considered to be located in the x-z plane.

DOI: 10.13009/EUCASS2017-146

Phase change modelling is done with the Hertz-Knudsen model by Collier and Thome (1999) [11] which is the standard model used in FLOW-3D. The phase change mass flow is calculated with the following formula:

$$\dot{m} = \alpha \cdot \sqrt{\frac{M}{2\pi RT}} \left(p_{sat} - p_{vapor}\right) \quad \textbf{(1)}$$

, where

- p_{vapor}: partial pressure of the vapor in the gaseous fluid;
- p_{sat} : saturation pressure at the local temperature, computed from the Clausius-Clapeyron equation;
- α : so-called accommodation coefficient;
- R : gas constant, M: molar mass, T: mean temperature in the calculated mesh cell;
- $\dot{m} > 0$ denotes evaporation, $\dot{m} < 0$ denotes condensation.

The accommodation coefficient limits the phase change within the boundary layer at the liquid/gas interface. The coefficient's value is generally lower or equal than 1. A priori the coefficient is not known and has to be found based on experimental results. In the present study the value was set to $\alpha = 0.001$.

The initial flow conditions were set with a pre-run at 1g gravity conditions to obtain the appropriate wetting conditions at the dewar walls. The pre-run duration was 0.25 seconds which was kept short to reduce disturbances of the initial temperature distribution. Furthermore the liquid viscosity was artificially increased by a factor of 10 to improve the stability of the free surface at the time of step reduction in gravity. Phase change was neglected for the pre-run. The conditions at start of the pre-simulation and the conditions at the time of the final simulation are shown in Figure 3.

5 Results

5.1 Global behaviour

The following figures compare the different numerical solutions for cases 1 and 2. Figure 4 compares simulations for case 1 showing the reorientation behaviour of the 1-fluid model and the 2-fluid model depicting velocities.

Time (s)	Case 1 Velocity magnitudes (m/s)			
	1-fluid model 3D view	1-fluid model 2D view (xz axis)	2-fluid model 3D view	2-fluid model 2D view (xz axis)
1	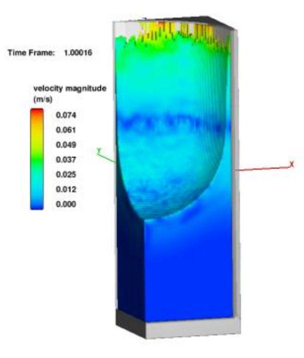	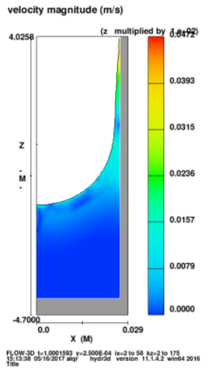	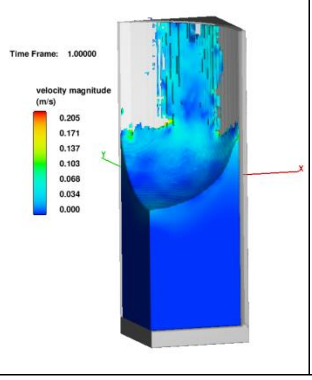	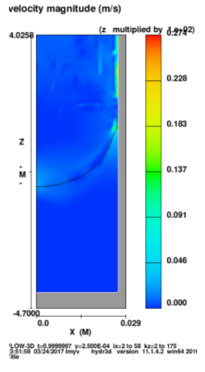

DOI: 10.13009/EUCASS2017-146

1.5	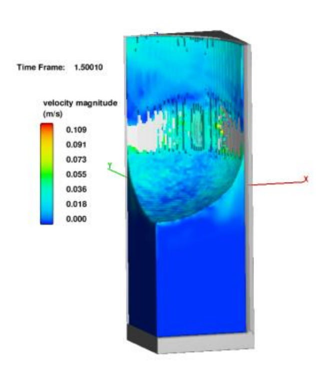	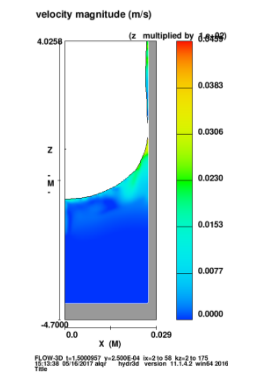	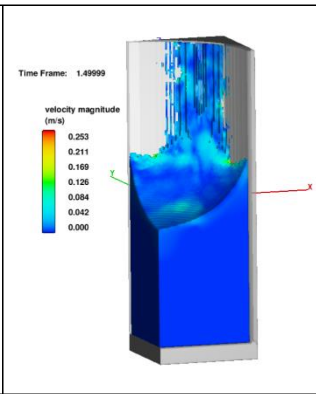	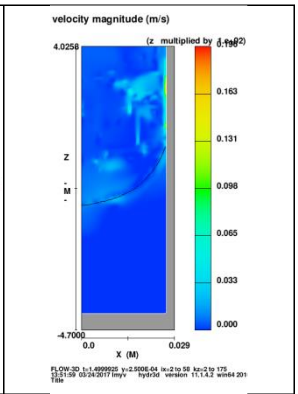
2	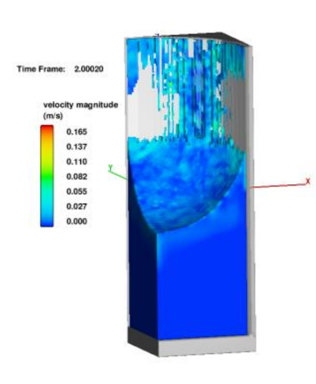	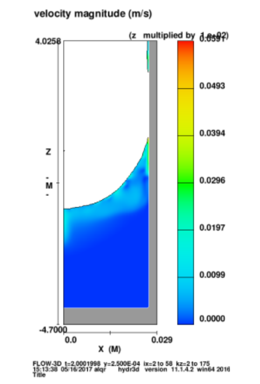	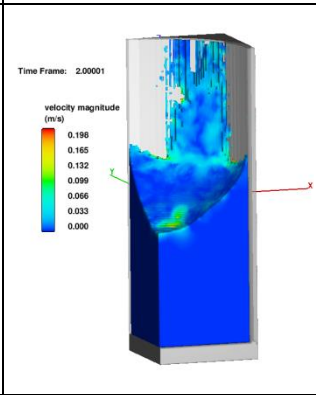	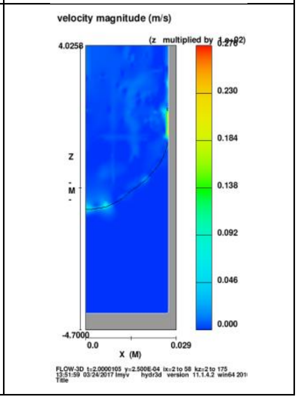

Figure 4: Comparison of the reorientation process concerning experiment case 1 comparing the 1-fluid and the 2-fluid approach.

It can be seen that the 1-fluid model (left column) considers a wetting layer moving up the tank walls which separates from the bulk liquid. This liquid layer formation is well known and is also reflected in [5]. The wetting conditions are however not rotational symmetric over the circumference which appears to be driven by the rectangular grid. The 2-fluid model (right column) does not show the generation of this wetting layer. The contact line appears to be pinned at t = 2 seconds. Thus modelling of the contact line appears to differ between the 1-fluid and the 2-fluid model. The 1-fluid model is however more representative.

Figure 5 compares simulations for case 2 showing the reorientation behaviour of the 2-fluid model under isothermal conditions and non-isothermal conditions.

Time (s)	Case 2 Temperatures (K)			
	Without phase change		With phase change	
	3D view	2D view (xz axis)	3D view	2D view (xz axis)
0.5	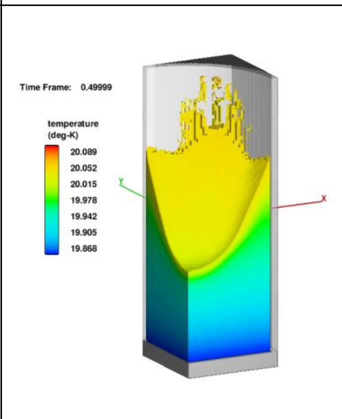	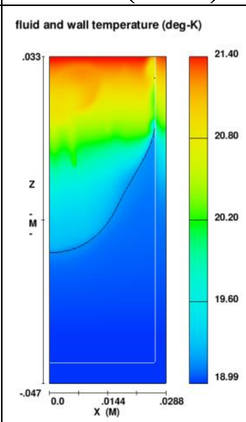	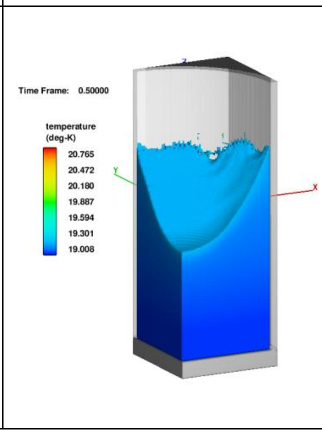	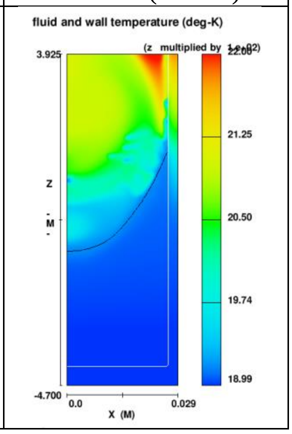

DOI: 10.13009/EUCASS2017-146

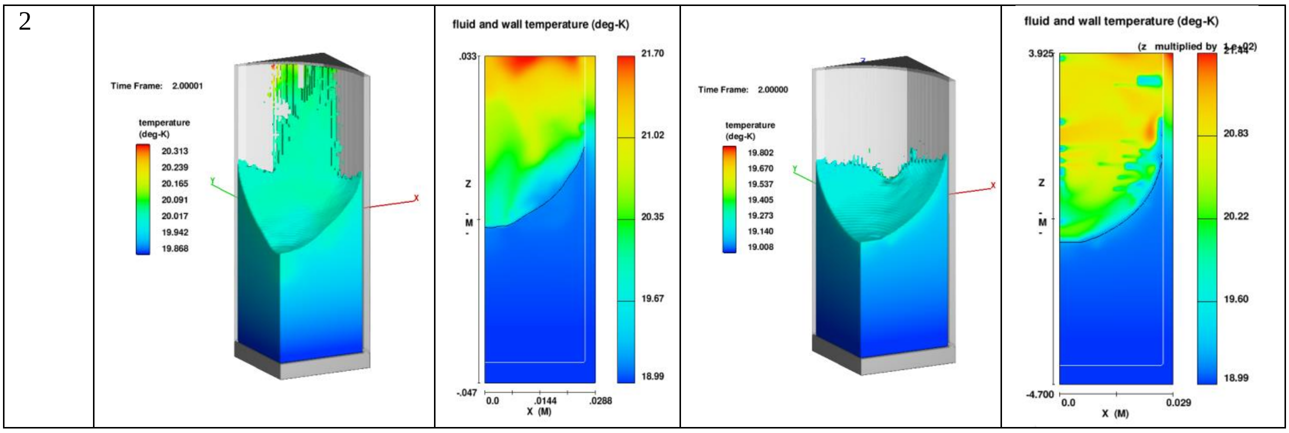

Figure 5: Comparison of the reorientation process concerning case 2 without phase change (left columns) and with phase change (right columns).

For case 2 computations, same as in case 1, the wetting conditions change along the circumference. A wetting layer formation is partially visible in the model without phase change which appears to diminish when phase change is considered. Again the rectangular grid appears to impact the wetting conditions of the wall.

5.2 Comparison of the free surface elevations

In the present chapter the centre point free surface movements of the experimental and the numerical results are compared. The following figures show the different centre line deflections for experiment cases 1 and 2.

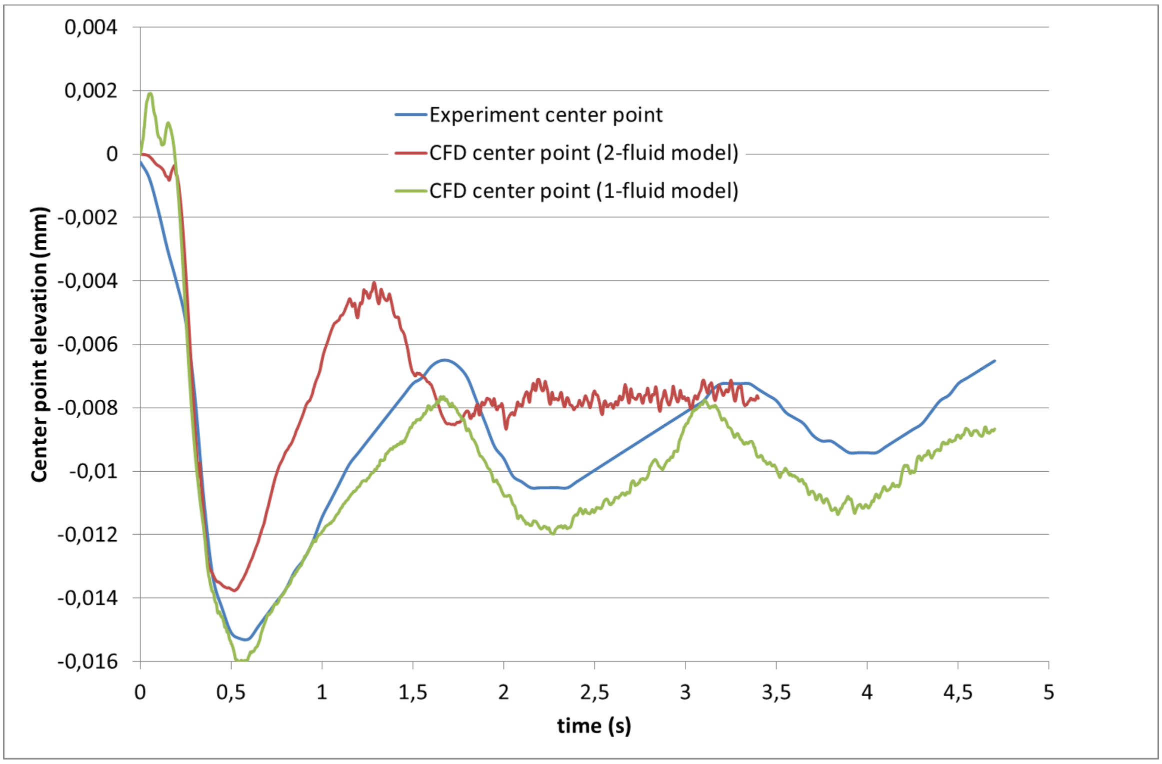

Figure 6: Case 1: Centre point movement with respect to time without phase change: blue: experiment; green: CFD with 1-fluid model; red: CFD with 2-fluid model

DOI: 10.13009/EUCASS2017-146

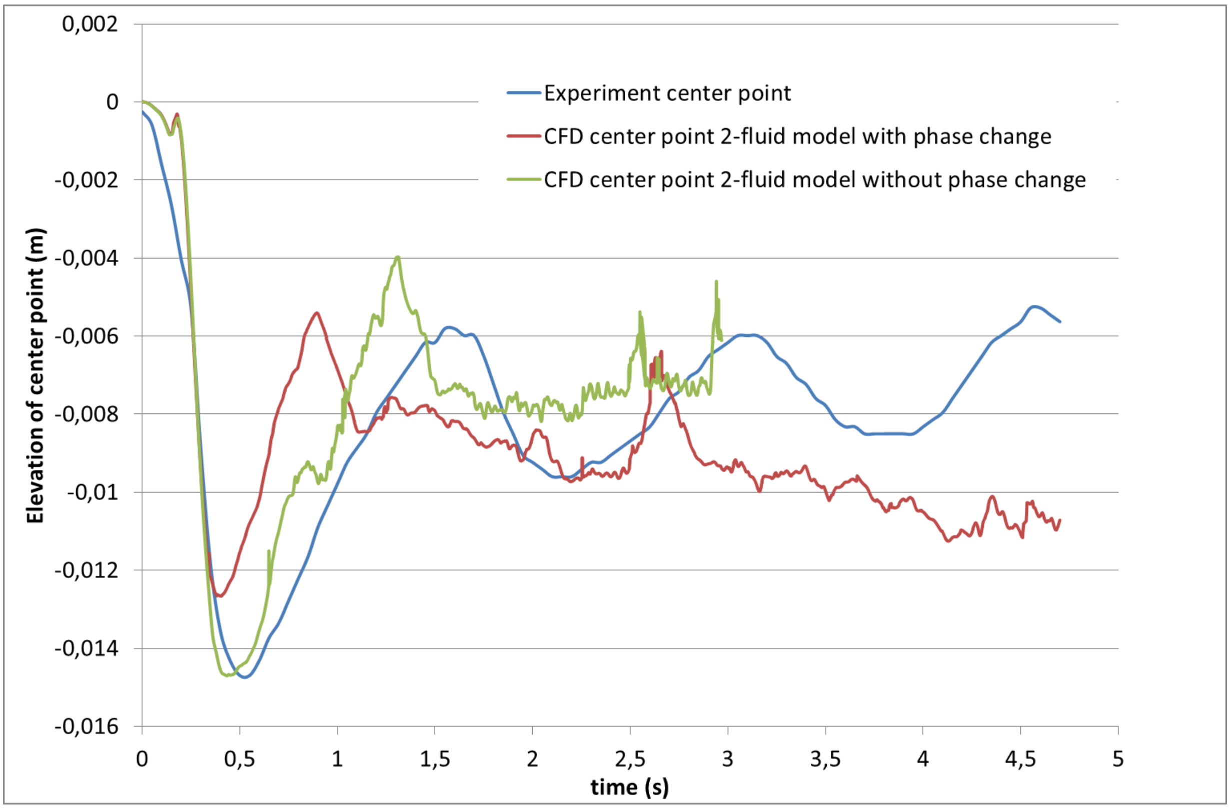

Figure 7: Case 2: Centre point movement with respect to time: blue: experiment; green: CFD with 2-fluid model without phase change; red: CFD with 2-fluid model including phase change

It can be seen that the 1-fluid model, which does not take into account any thermal effects, is able to reflect the reorientation behaviour of the free surface very well. Also the oscillations are shown which occur after about 1 second of 0g. The 2-fluid model however does not reflect these oscillations. The 2-fluid model does not generate a similar wetting of the tank wall. In contrast to the 1-fluid model the contact line is pinned after the first oscillation which hinders oscillations of the centre point free surface. These oscillations are visible in both experiment cases 1 and 2. In this context the 2-fluid model is not representative to the experiment.

5.3 Comparison of temperature sensor data

For the measured temperatures, an accuracy of the experimental data of ±0.25K was taken into account according to [8]. The following tables 3 and 4 summarize the temperature conditions in the beginning and the end and the corresponding temperature changes over the free fall for cases 1 and 2.

It can be seen that all temperature sensor readings of case 1 deviate within the accuracy limit during the time of the free fall. This is as expected since case 1 concerns the isothermal temperature conditions without significant temperature gradients. All temperature readings are therefore considered as isothermal. The numerical results reflect this isothermal behaviour. The maximum deviation between experiment and numerical results is -0.26K which is still about the sensor accuracy.

Concerning case 2 (Table 4) sensors T_{WL1}, T_{WL2}, T_{WIF} and T_{WV1} are also in the range of the temperature accuracy. The numerical results also show an accuracy threshold in the range of the sensor accuracy. All other temperature measurements are discussed in more detail in the following.

DOI: 10.13009/EUCASS2017-146

Table 3 Temperature sensor conditions in the beginning and the end and the corresponding temperature changes over the free fall for cases 1

Sensor	Experiment			Numeric				Remark
	Initial temp	Final Temp	Change at t=4.7s	Temperature at t=0s	Temperature at t=4.7s	Offset between experiment & numeric at t=0s	Offset between experiment & numeric at t=4.7s	
T_{WL1}	19.89	20	0.11	19.89	19.89	0	-0.11	below threshold
T_{WL2}	19.98	20.09	0.11	19.98	19.98	0	-0.11	below threshold
T_{WIF}	20.06	20.1	0.04	20.05	20	-0.01	-0.1	below threshold
T_{WV1}	20.04	20.11	0.07	20.04	20.01	0	-0.1	below threshold
T_{WV2}	20.03	20.13	0.1	20.03	20.04	0	-0.09	below threshold
T_{WV3}	20.02	19.85	-0.17	19.99	20.05	-0.03	0.2	below threshold
T_{WV4}	20.13	20.33	0.2	20.05	20.07	-0.08	-0.26	below threshold
T_{WV5}	20.02	20	-0.02	20.05	20.14	0.03	0.14	below threshold
T_{V1}	20.03	20.28	0.25	20.04	20.11	0.01	-0.17	below threshold
T_{V2}	20.06	20.32	0.26	20.07	20.23	0.01	-0.09	below threshold
T_{V3}	20.2	20.48	0.28	20.02	20.28	-0.18	-0.2	below threshold
T_{V4}	21.24	21.33	0.09	21.36	21.4	0.12	0.07	below threshold

Table 4 Temperature sensor conditions in the beginning and the end and the corresponding temperature changes over the free fall for cases 2

Sensor	Experiment			Numeric				Remark
	Initial temp	Final Temp	Change at t=4.7s	Temperature at t=0s	Temperature at t=4.7s	Offset between experiment & numeric at t=0s	Offset between experiment & numeric at t=4.7s	
T_{WL1}	19.03	19.26	0.23	19.03	19.03	0	-0.23	below threshold
T_{WL2}	19.12	19.37	0.25	19.12	19.12	0	-0.25	below threshold
T_{WIF}	19.2	19.4	0.2	19.21	19.15	0.01	-0.25	below threshold
T_{WV1}	19.48	19.41	-0.07	19.49	19.29	0.01	-0.12	below threshold
T_{WV2}	19.85	19.4	-0.45	20	19.71	0.15	0.31	above threshold
T_{WV3}	20.25	19.55	-0.7	20.59	20.21	0.34	0.66	above threshold
T_{WV4}	20.76	20.03	-0.73	21.03	20.66	0.27	0.63	above threshold

DOI: 10.13009/EUCASS2017-146

T_{WV5}	21	19.8	-1.2	21.08	19.8	0.08	0	above threshold
T_{V1}	20.16	21.33	1.17	20.16	20.79	0	-0.54	above threshold
T_{V2}	21.78	22.62	0.84	20.79	21.23	-0.99	-1.39	above threshold
T_{V3}	21.38	21.76	0.38	21.42	21.02	0.04	-0.74	above threshold
T_{V4}	24.47	24.68	0.21	24.53	22.59	0.06	-2.09	above threshold

In the following figures only those sensor temperatures are compared which show a change in temperatures above the sensor accuracy of ±0.25K.

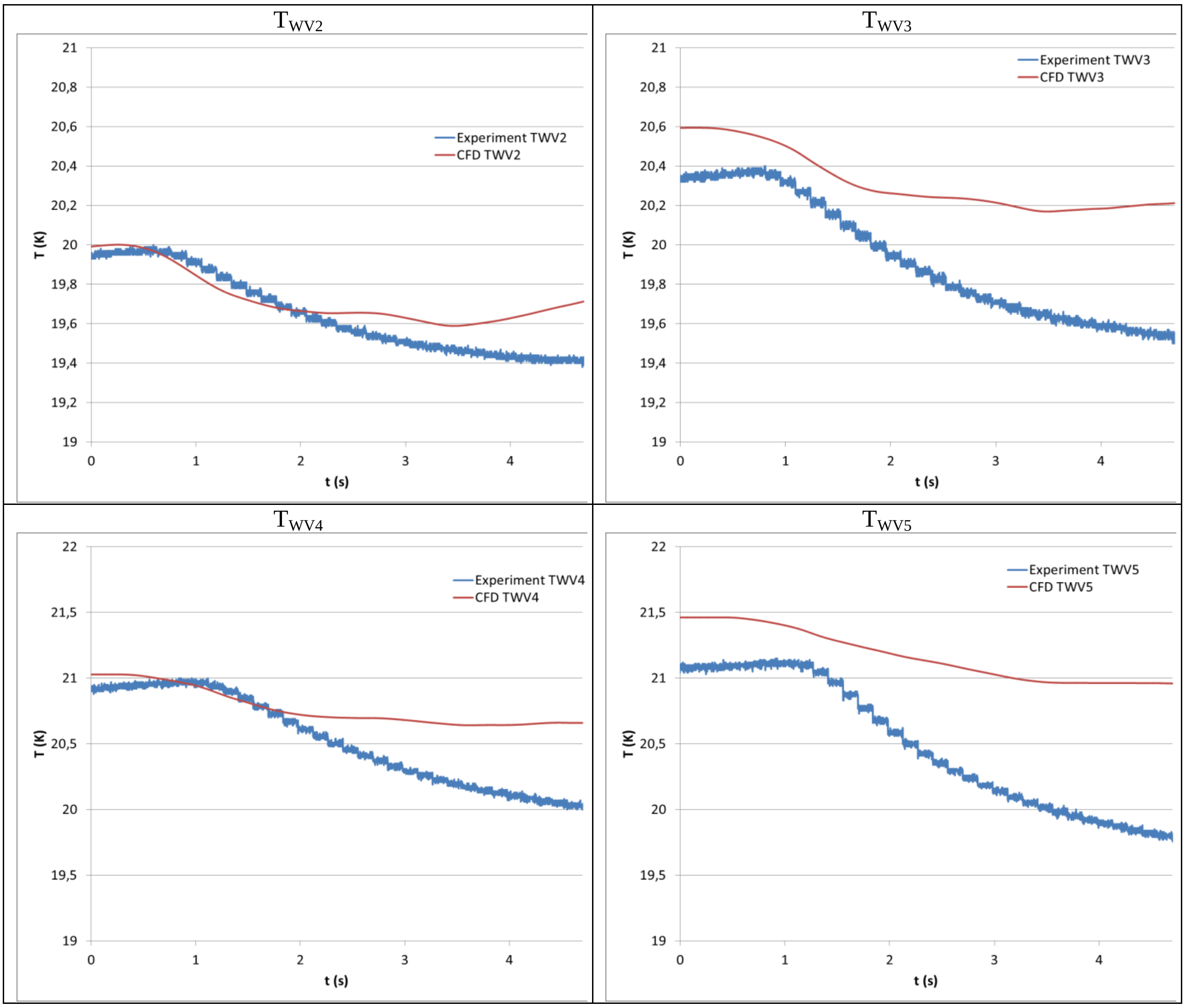

DOI: 10.13009/EUCASS2017-146

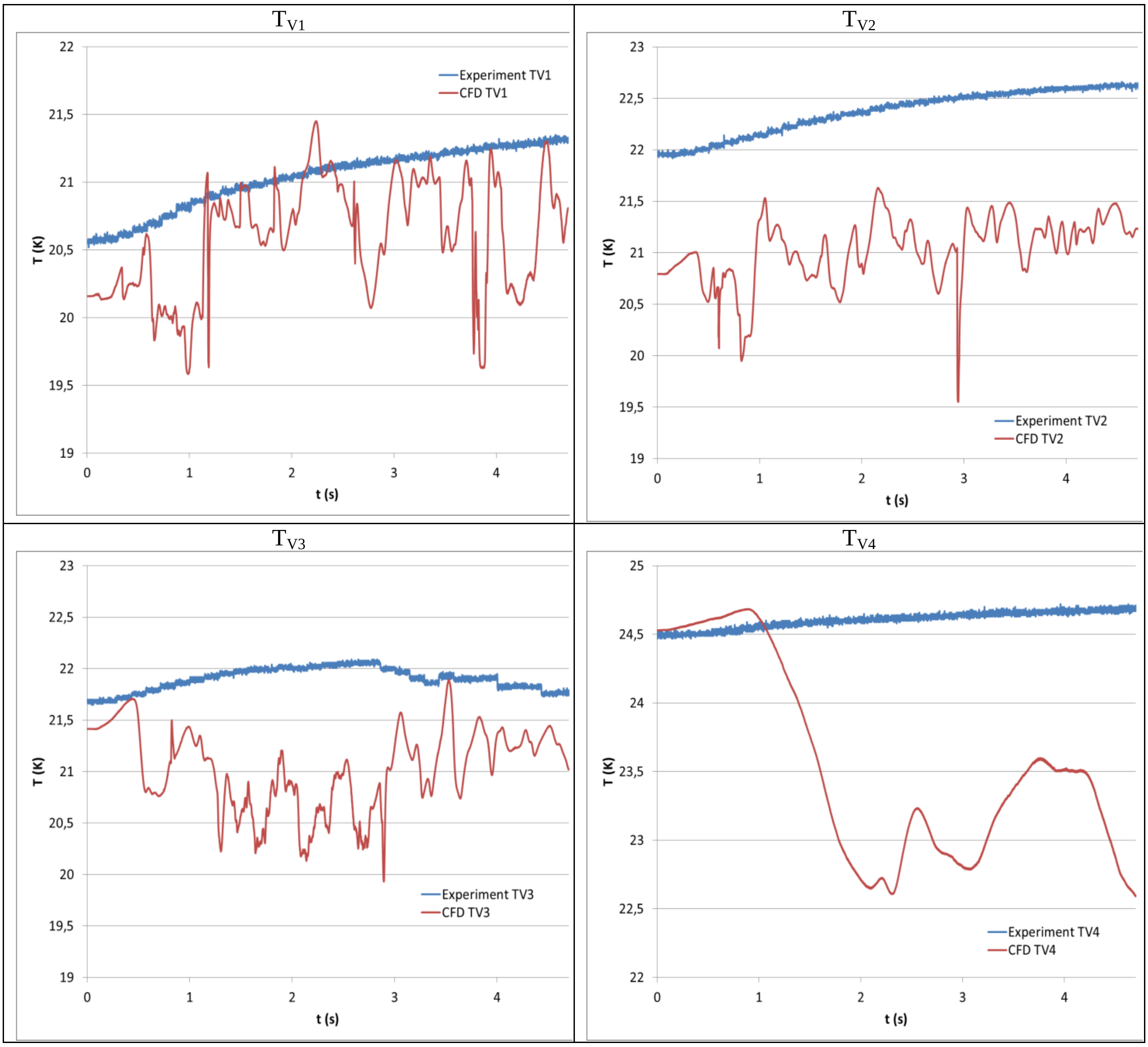

Figure 8: Case 2 - Comparison of temperature sensor data between experiment and numerical analysis considering phase change

Temperature sensors T_{WV2} to T_{WV5} are initially in the vapour phase. They start cooling down, driven by the reorientation of the cooler liquid. This trend is also observed in the numerical analyses. The drop in temperature is however more pronounced in the experimental results.

Temperature sensors T_{V1} to T_{V4} are placed inside the dewar in the gas phase. The numerical results for T_{V1} to T_{V3} show much higher fluctuations compared to the experiment. T_{V1} and T_{V2} follow the trend of the temperature evolution. T_{V2} is however 1K off at t=0s which stays in the same range over the time of the drop.

T_{V4} deviates considerably from the experimental results. The sensor is placed above the field of view near the flange interface. It is expected that the thermal condition of this region is not considered representative enough in the numerical analysis.

DOI: 10.13009/EUCASS2017-146

5.4 Comparison of the pressure history

The comparison of the pressure history profiles are shown in Figure 9.

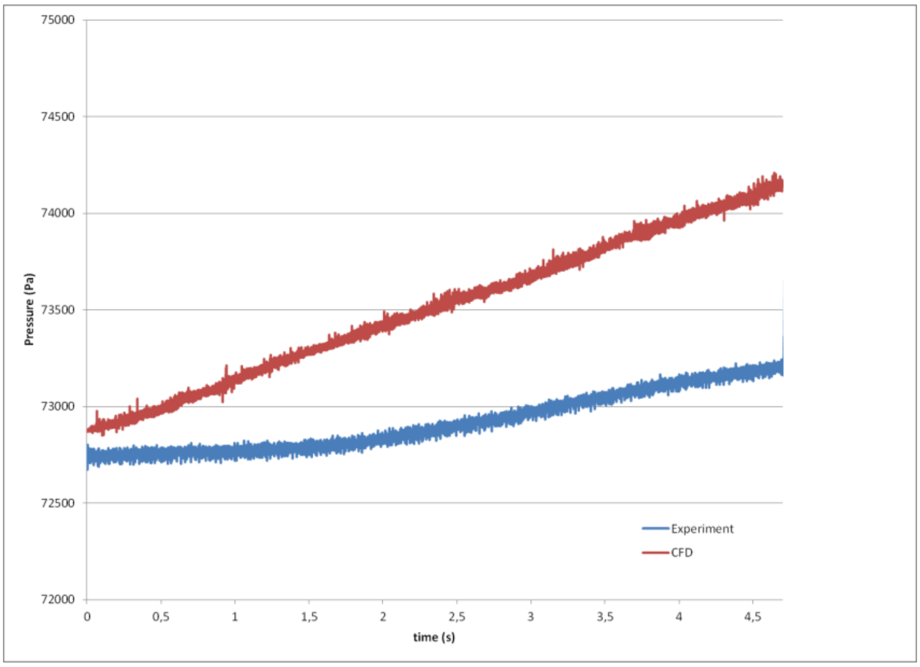

Figure 9: Case 2: pressure history (blue: experimental result; red: CFD analysis considering phase change)

The numerical result (in red) shows a linear rise in pressure while the rise in pressure appears to be delayed in the experiment. The experiment shows that the pressure starts to rise after about 1-1.5 seconds. The pressure rise is in the numerical analysis higher than in the experiment. Further analyses, tuning the sizing coefficient in combination with the numerical grid would be necessary.

6 Conclusion

The present document presents a comparison between experiment and numerical analysis concerning the reorientation of liquid hydrogen after a step reduction in gravity. Different initial temperature and pressure conditions were compared to experimental results. The following conclusions can be drawn from these comparisons, using the CFD software FLOW-3D®:

- Under isothermal conditions, using a 1-fluid model, the movement of the free surface can be well modelled.
- In all simulated CFD analyses the contact line motion is not symmetric over the circumference which appears to be driven by the rectangular grid model. This aspect should be improved.
- Most of the temperature sensors compare well. The drop in temperature is detected by the numerical analysis for the non-isothermal experiment (case 2). However the drop in temperature in the wall appears to be lower than in the experimental results. This may be driven by differences concerning wall wetting. The temperature in the solid drops when adjacent cooler liquid leads to a temperature drop. If the wetting conditions are differing then the drop in temperature will also differ. In conclusion a more accurate representation of the contact angle is needed for the 2-fluid model.
- An alternative phase change model would also be beneficial which is not depending on an a priori unknown scaling factor. In this context models discussed in [12] by Kunkelmann could be an option improving phase change modelling for the Volume of Fluid method.

DOI: 10.13009/EUCASS2017-146

Acknowledgement

This work is funded by the German Federal Ministry of Economic Affairs and Energy (contract code: 50RL 1620) and administered by the German Space Agency (DLR). Their support is greatly appreciated.

Supported by:

Federal Ministry for Economic Affairs and Energy

on the basis of a decision by the German Bundestag

DLR

References

[1] Tam, W., Behruzi, P., Jakle, D., and Netter, G. 2016, The Evolutionary Forces and the Design and Development of Propellant Management Devices for Space Flight in Europe and the United States, *Space Propulsion Conference*.

[2] Fuhrmann, E. Dreyer, M. E. 2009, Heat Transfer by Thermo-Capillary Convection, *Microgravity Sci. Technol*., 21, pp. S87-S93.

[3] Konopka, M., Behruzi, P., Schmitt, S., and Dreyer, M. E. 2014, Phase Change in Cryogenic Upper Stage Tanks, *AIAA Propulsion and Energy Conference*, AIAA 2014-3994.

[4] Behruzi, P., Klatte, J., Schütte, A. Schmitz, B., and Köhler, H. 2013, Cryogenic Propellant Management Sounding Rocket Experiments on TEXUS 48, *49th AIAA/ASME/SAE/ASEE Joint PropulsionConference*, AIAA 2013-3904.

[5] Kulev, N., and Dreyer, M. 2010, Drop Tower Experiments on Non-isothermal Reorientation of Cryogenic Liquids, *Microgravity Sci.Technol.*, 22:463-474.

[6] Bänsch E. 2001, Finite element discretization of the Navier–Stokes equations with a free capillary surface. *Numer. Math.*, 88:203–35.

[7] Kulev, N., Basting, S., Bänsch, E., Dreyer, M. 2014, Interface reorientation of cryogenic liquids under non-isothermal boundary conditions, *Cryogenics*, 62, 48-59

[8] Schmitt, S., and Dreyer, M. E. 2015, Free surface oscillations of liquid hydrogen in microgravity conditions, *Cryogenics*, 72, 22-35

[9] Eckels P. 2009, Cryocomp, Software CryoComp, Version 5.0.

[10] Lemmon EW, Peskin AP, McLinden MO, Friend D. 2010, NIST thermodynamic and transport properties of pure fluids – NIST pure fluids. Software. NIST Standard Reference Database, 23, Version 9.0.

[11] Collier, J. G., Thome, J. R. 1999, Convective Boiling and Condensation, *Oxford Science Publications*.

[12] Kunkelmann, C. 2011, Numerical Modeling and Investigation of Boiling Phenomena, PhD Thesis, Technical University Darmstadt